

# Gating system design to cast thin wall ductile iron plates

P. David, J. Massone, R. Boeri and J. Sikora\*

The present study describes the development of a horizontal and a vertical mould designed to produce thin ductile iron plates of 1.5–4 mm thickness. Both moulds used a non-pressurised configuration. The horizontal mould design was based on empirical rules, while the vertical mould was based on numerical simulations of fluid flow and thermal field, carried out using the software NovaFlow&Solid. The aim of both designs was to produce sound ductile iron plates that were large enough to make tensile test samples. The results show that the adoption of empirical rules and a non-pressurised configuration were not enough to guarantee proper filling. An optimised design was obtained through the use of mathematical modelling.

**Keywords:** Ductile iron, Thin wall, Mould design

## Introduction

All industries involved in the production of structural parts and machine components face a sustained call for the development of lighter and stronger products. This demand is particularly intense in the automotive industry, where there is an increasing need to save fuel and to reduce the emissions of carbon dioxide. The typical candidate materials to produce large amounts of light parts should have high strength and stiffness, be of low density, and very important, must be produced in large quantities at low costs. Light metal alloys and composites have claimed most of the light components market. Nevertheless, the continuous search for new alternatives has recently focused attention on the development of technologies that allow the production of ductile iron (DI) parts as thin as 2 mm, known generally as thin wall ductile irons (TWDI). A first look at the properties of DI shows two major factors that appear to limit its application to light parts: (i) DI is not a low density alloy and (ii) DI is difficult to shape into thin wall parts. On the other hand, DI offers several favourable features: it can be produced by casting in large amounts at low cost, there are plenty of facilities to produce ductile iron castings, it has high stiffness, and it can reach very high strength by heat treatment. In fact, when heat treated to reach high strength, DI shows strength to density and stiffness to density ratios that are comparable to those of conventional light alloys. To make full use of these favourable features in the construction of light components, it has to be possible to cast thin wall DI parts. The industrial production of DI is generally limited to parts having a wall thickness above 5 mm. Significant research efforts have

been recently devoted to the development of TWDI technology.<sup>1–5</sup>

The use of conventional melting and pouring practices to cast DI in sand moulds faces progressive inconveniences as the thickness decreases. The most significant problems are the formation of microshrinkage cavities and the precipitation of carbides. Microshrinkage is the result of improper feeding, whereas carbide precipitation is caused by a high cooling rate. Proper feeding requires an efficient mould design, whereas the control of carbide precipitation requires the use of specific melt compositions, and proper inoculation practice and casting procedures.

The selection of a proper melt composition to produce TWDI has received some attention in the literature.<sup>2–5</sup> Most results conclude that hypereutectic unalloyed DI is best suited to obtain sound parts.

The design of moulds for TWDI has received less attention. Nevertheless, this is particularly critical, since the presence of small defects that are negligible in large castings can cause the rejection of a thin wall part.

The main criteria to be fulfilled by a gating system are: (i) the melt must flow through the different parts of the gating system with minimum turbulence to avoid metal oxidation, gas entrapment and inclusions as a result of mould erosion and slag entrapment; (ii) the melt must enter the mould in a manner that allows the solidification to advance from the part to the risers or feeder heads. Different authors advise the use of a large number of empirical rules to satisfy these criteria. Many times these rules are conflicting and lead to very different gating system designs. An example of the wide differences existing among authors is made evident by the fact that the use of both pressurised and non-pressurised gating systems is advised for the casting of similar parts.<sup>6–8</sup>

Several authors have designed moulds to produce thin DI plates as part of their research on the metallurgy of TWDI. Labrecque and Gagné<sup>9</sup> report the production of

Faculty of Engineering, Metallurgy Division, INTEMA, National University of Mar del Plata – CONICET, Av. Juan B. Justo 4302, B7608FDQ Mar del Plata, Argentina

\*Corresponding author, email jsikora@fi.mdp.edu.ar

carbide-free 3 mm thick ductile iron plates. They used a hypereutectic DI and a two-step inoculation process including Bi-bearing ferrosilicon as a late inoculant. The mould was designed by applying conventional rules, and optimised by software simulations of filling. The design of the gating system aimed to minimise the turbulence. The vertical moulds used were made of AFS GFN 75 chemically bonded silica sand and included ceramic filters. The study concentrated on the evaluation of the microstructure. The results showed that the microstructure is largely affected by the plate thickness, and the authors suggest that design criteria for TWDI must be based on the thinnest section of the casting.

Stefanescu and coworkers<sup>2,3</sup> studied the production of TWDI plates using a horizontal mould. A large fraction of the plates cast using this mould showed solidification defects that were associated with deficiencies in feeding and fluid flow. In an attempt to minimise defects, a new mould was designed, using a vertical configuration. The design allowed vertical plates to be filled from the bottom, and included a ceramic filter and proper risers. The runner fed cylindrical risers, and these risers fed three thin plates of 6, 2.5 and 3.5 mm thickness from bottom to top. Stefanescu and colleagues pointed out the importance of the use of numerical simulations to assist in the design of gating systems for TWDI.

Mampaey and Xu<sup>10</sup> also designed a vertical mould to cast 3 mm thick DI plates. The gating system design was optimised by mathematical modelling of fluid flow, and was also validated by observation of the fluid flow during filling by using moulds that included transparent heat-resistant windows. A large difference in temperature between the top and the bottom of the plates was observed during filling. This had a marked influence on the subsequent solidification. Therefore, reliable simulations of TWDI castings must take into account the heat transfer during the filling stage.

Several studies focused on the mechanical properties of TWDI.<sup>2,11,12</sup> Stefanescu *et al.*<sup>2</sup> found large variations in the strength and elongation of TWDI cast using similar conditions. The dispersion in the values seemed to be caused by microstructural anomalies generated during solidification, such as microshrinkage, graphite and dendrite alignment, inverse chill and oxide particles. Labrecque *et al.*<sup>11</sup> measured the mechanical properties of ductile irons cast in sections of 3 and 10 mm. The tensile strength and elongation of samples taken from the 10 mm thick plates satisfied the requirements of ASTM A 536, while samples from the 3 mm thick plates showed lower and more dispersed values that failed to satisfy the standards in most cases.

Javaid *et al.*<sup>12</sup> also found dispersed values of the mechanical properties of TWDI. Acceptable mechanical properties, satisfying ASTM A 536, were found when the material showed good nodularity, high nodule counts and a matrix free from carbides and inclusions. On the other hand, samples that failed to satisfy the standards showed microstructural anomalies.

Stefanescu *et al.*<sup>3</sup> showed that the strength and elongation of TWDI are largely influenced by the surface roughness and the graphite morphology. Poor properties of TWDI were found to be associated with low nodularity and coarse surface roughness. Testing of samples having the original casting skin showed that when roughness values exceeded  $R_a=10\text{ }\mu\text{m}$ , a

pronounced decrease in strength and elongation was observed. Samples in which the casting skin had been removed by grinding showed consistently higher tensile properties.

The literature shows that TWDI has the potential to satisfy the requirements of the standards devised for regular DI. Nevertheless, many studies showed a significant proportion of samples that failed to satisfy the minimum requirements of ASTM A 536. Unsatisfactory properties were generally linked to casting defects. This large dispersion in properties makes it difficult to carry out studies on the mechanical properties of TWDI and the influence of several variables on them. Therefore, it becomes critical to study the criteria to design TWDI moulds, and to design moulds that can produce sound TWDI parts consistently.

Some of the microstructural problems that affect the mechanical properties of TWDI appear to be linked to the design of the gating systems. Most designs have been based on rules devised for thick parts. Some of these designs needed adjustments to control fluid flow.

The present study describes the development of horizontal and vertical gating system designs to produce 1.5 to 4 mm thick ductile iron plates. The design process was accompanied by numerical simulations of fluid flow and thermal field carried out using the software NovaFlow&Solid. The aim of the design was to produce plates of sound DI that were large enough to make testing samples. These samples are necessary to perform future studies aimed at characterising TWDI properties, and to analyse the influence of the matrix microstructure and the nodule morphology and size on the properties.

The ability of the vertical and horizontal moulds to produce sound TWDI plates will be assessed by measuring the tensile properties of samples taken from plates of different thickness cast using those moulds.

## Experimental methods

The first mould was designed using a horizontal configuration, following empirical rules reported in the literature and prior knowledge of the authors. This configuration was later analysed using simulation software NovaFlow&Solid version 2.9.

The second design used a vertical arrangement, and was carried out using careful calculations of fluid flow done with NovaFlow&Solid. The aim was to maintain a very low turbulence and to obtain a progressive filling of the plates, following the recommendations of Campbell.<sup>7,13</sup>

NovaFlow&Solid applies the finite element method to calculate fluid flow and solidification. Thermophysical data included in the software database were used to simulate the casting and mould materials. The size of the finite element cells was small enough to include at least three elements in the thinnest casting section, as suggested by the software provider. Air gap formation was not accounted for in the modelling. Filters were modelled using multi layers with a filter factor of  $1\text{ m s}^{-1}$ . The filter thickness was 13 mm.

The moulds were prepared using AFS GFN 60 silica sand bonded by 1% of an alkyd-urethane resin system (alkyd-urethane system: Part A, alkyd type resin=1% sand weight; Part B, liquid amine catalyst, =5% part A; Part C: isocyanate, the urethane component, =20% part

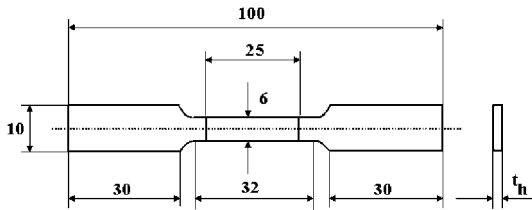
A). No mould wash was used on the cavity of the thin plates. Graphite paint was applied on the sprue and the well to minimise mould erosion.

The melts were prepared using a 50 kg capacity medium frequency induction furnace. The charge materials were pig iron, steel scrap, recarburiser and ferrosilicon. The melts were superheated to 1540–1550°C. The melt was treated in two stages, using separate ladles. Nodularising was carried out by applying the sandwich method in the first ladle, and using 1.2% of FeSiMg (6%). Post-inoculation was carried out in the second ladle using 0.65% of FeSi (75%Si, 1.1%Ca) in the stream. The pouring temperature ranged between 1320 and 1350°C.

Vertical and horizontal moulds were used to obtain eight vertical plates and eight horizontal plates of two unalloyed melts. The chemical compositions and the Carbon Equivalent (CE) values are listed in Table 1. The chemical compositions of both heats were hyper-eutectic. The CE values of Melts A and B aimed at following the recommendation of an earlier study, which showed that the best mechanical properties of TWDI are obtained for hypereutectic irons having CE values below 4.6%.<sup>14</sup> Melt B showed a CE value slightly greater than the limit, but was still considered suitable for the study.

Although as cast plates microstructures were predominantly ferritic, noticeable amounts of carbides were present near the edges of the plates, and some differences were observed in the amount of pearlite and carbides depending on the plate thickness. Therefore all plates were fully ferritised before mechanical testing in order to homogenise the matrix microstructure.<sup>14</sup> This was done by austenitising at 910°C during 2 h followed by furnace cooling to room temperature. Samples were protected against decarburisation by using a pack of cast iron turnings and coal. After being ferritised, the plates were cut and used to prepare flat tensile samples of 100 mm × 10 mm × plate thickness (*th*), according to ASTM E 8M (Fig. 1). The casting skin of the tensile samples was removed by grinding a depth of approximately 0.2 mm off each face. The resulting thicknesses of the tensile samples taken from the 4, 3, 2 and 1.5 mm plates were then 3.6, 2.6, 1.6 and 1.1 mm, respectively. Tensile tests were carried out using an Instron 8501 machine.

The micro and macrostructures of the thin wall plates were characterised using conventional polishing and etching techniques. The characterisation of the microstructure involved the quantification of the nodule count and morphology in different sections of the plates, and the identification of microshrinkage cavities through the entire casting. Nodule counts were measured on unetched polished samples using the Image Pro Plus software. The graphite morphology was characterised by measuring the sphericity and nodularity on the 2 and 4 mm plates from the vertical mould. Sphericity (*Sph*) values were calculated from readings of area and



1 Scheme of tensile test samples (dimensions in millimetres)

perimeter of nodules measured using the Image Pro Plus software. Digital images were obtained using an STC-60 video camera and a PV-CL544XP11 video board. A threshold value of 5 µm was used for the diameter of the particles accounted as nodules. *Sph* was calculated using the following expression

$$Sph = \frac{4 * \pi * Area}{Perimeter^2}$$

Reported values are the average of three readings per sample.

Roughness measurements were carried out using a Surtronic 3+ roughness meter on the face of horizontal plates. Reported values are the average of at least three readings.

Results

Design of horizontal mould gating system

The aim of the design was to provide plates that allowed four tensile test samples to be obtained. A coupon of 100 mm × 60 mm × *th* is required to machine four tensile samples of the dimensions shown in Fig. 1. The excess in the width is necessary to allow sectioning. The question was whether a plate of this thickness can be cast using gravity casting and a horizontal mould configuration.

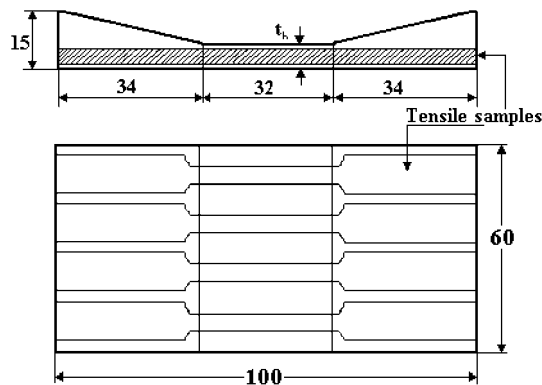
Campbell<sup>7</sup> reviews the subject, and quotes work of Pellini *et al.*, that states that a feeder linked to a plate can effectively feed a distance of twice the thickness of the plate. Although this rule was derived for thick steel plates (50–200 mm) cast in sand moulds, it has been extensively applied to other materials and dimensions. Ductile iron shows better feeding characteristics than steel, nevertheless, values characterising the feeding ability of risers for ductile iron were not found. Therefore, the rule of Pellini can be used for a first approximation.

Accordingly, a 1.5 mm thick plate surrounded by two feeders could have a maximum width of only 6 mm. This is much smaller than the 60 mm required, and it suggests that such a casting cannot be produced. Nevertheless, practical experience on DI casting suggests that the feeding distance limit is larger for the particular case of thin wall castings.<sup>7</sup>

The casting used to obtain the coupon can have the shape shown in Fig. 2. This shape only includes a thin central portion, wide enough to accommodate the length of the gauge section of the tensile samples, of 32 mm, which is the volume of metal effectively tested and this is the region that must display a microstructure typical of the thin wall material. The thin portion of 32 × 60 mm is in contact with two truncated wedge shaped risers. The bottom side of the casting is entirely flat to facilitate machining.

Table 1 Chemical composition of melts

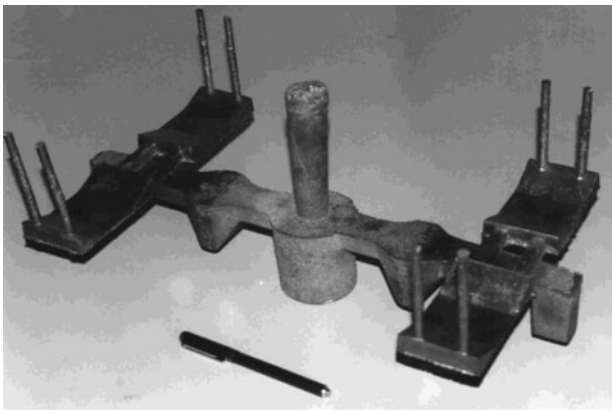
| Melt | Chemical composition, wt-% |      |      |       |       |       |      |
|------|----------------------------|------|------|-------|-------|-------|------|
|      | C                          | Si   | Mn   | S     | P     | Mg    | CE   |
| A    | 3.53                       | 2.89 | 0.32 | 0.031 | 0.049 | 0.052 | 4.49 |
| B    | 3.65                       | 3.04 | 0.20 | 0.018 | 0.053 | 0.048 | 4.65 |



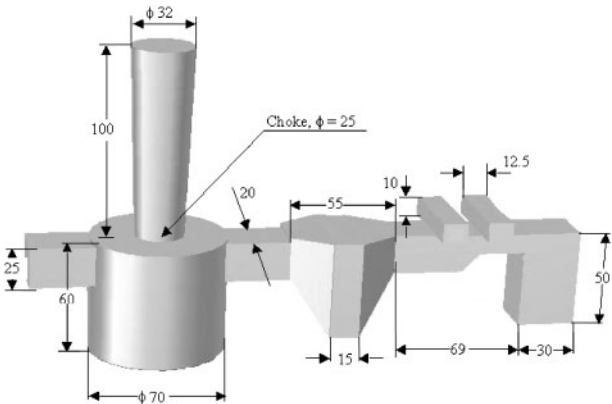
2 Shape and dimensions of block cast using horizontal mould (dimensions in millimetres)

Figure 2 shows the shape and dimensions chosen for the coupon to be cast using the horizontal mould and the sketch of the way in which tensile samples are taken from these coupons.

The next step in the development of the mould was to design a gating system that feeds an assembly of four coupons having 1.5, 2, 3 and 4 mm thick sections. All the design methodologies base the calculations on the size of the casting. In the case of thin wall castings, parts are generally small, and the calculations would lead to very small gating systems. Nevertheless, thin wall parts have a very small modulus, which increases the thermal gradients and demands very efficient filling and feeding, which are not always possible to obtain using small gating systems. Taking into account a casting that integrates four coupons as those shown in Fig. 2, the characteristic dimensions of the gating system can be calculated using different empirical criteria proposed in the literature, either based on the size of the parts or on its modulus. Table 2 lists the dimensions of the gating system of a horizontal mould containing four castings of 1.5, 2, 3 and 4 mm thickness, calculated using different empirical criteria. The differences in the characteristic dimensions of the moulds are very large. The recommendations for the ratio of the section areas of the different components of the mould (choke area/running area/ingate area) are particularly diverse. While some authors recommend the use of a pressurised gating system (2:1:1 ratio), others suggest the application of a non-pressurised configuration (1:4:4 ratio).<sup>6-8</sup> In view of the large differences in the recommended design criteria, the design of the horizontal mould was based on previous experience, using a non-pressurised configuration of 1:2:2 ratio. Ceramic foam filters were also used. Figure 3 shows a casting poured in the horizontal



3 Casting poured in horizontal mould



4 Schematic diagram of running and filter chambers in horizontal mould (dimensions in millimetres)

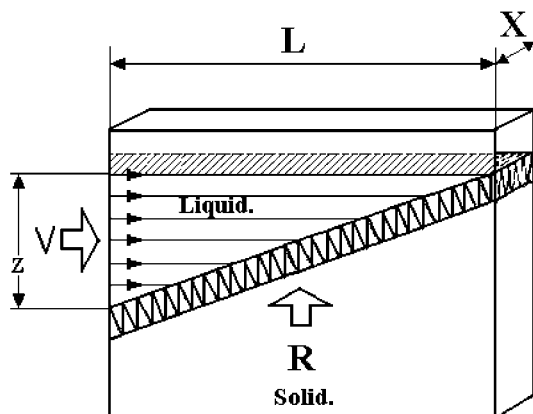
mould. Figure 4 shows a schematic diagram of one side of the horizontal mould running and filtering assembly. Table 3 lists the dimensions of the horizontal mould gating system.

Design of vertical mould gating system

The vertical mould was designed to yield two 100 × 60 mm plates, 2 and 4 mm thick. Its design follows the recommendations of Campbell and colleagues<sup>7,13,15</sup> for casting vertical plates, who state that the casting of a plate is more efficiently achieved when plates are set vertically, and the melt enters the cavity from the bottom to the top. If the vertical plate has vertical runners along its sides, connected by continuous ingates, filling can proceed slowly, without the usual requirement of completing the filling before solidification proceeds. The fluid flow can then be slow, and the surface

Table 2 Characteristic dimensions of gating system according to different authors

|   | Sylvia <sup>6</sup> | Campbell <sup>7</sup> | LaRue <sup>8</sup> |
|---|---------------------|-----------------------|--------------------|
| Height of sprue, mm   | 100                 | 100                   | 100                |
| Height of pouring basin, mm                                       | 70                  | 70                    | 70                 |
| Diameter at the top of the sprue, mm                              | ...                 | 3.9                   | ...                |
| Diameter of choke, mm   | 5.4                 | 3.6                   | 12.7               |
| Diameter of the sprue base, mm                                    | ...                 | 7.14                  | 28.4               |
| Height of the sprue base, mm                                      | ...                 | 19                    | 20.4               |
| Cross-sectional area of the runner (2), mm <sup>2</sup>           | 46                  | 135                   | 255                |
| Cross-sectional area of the individual gates (8), mm <sup>2</sup> | 11.5                | 67.5                  | 64                 |
| Ratio choke area/running area/ingate area                         | 1:4:4               | 1:27:54               | 1:4:4              |
| Length of the runner extension, mm                                | ...                 | ...                   | 60                 |



5 Schematic diagram of feeding sequence of vertical plate, as proposed by Campbell;<sup>13</sup> R, velocity of advance of solidification front; V, velocity of advance of liquid front; Z, height of rising liquid

turbulence is minimised. Additionally, this gradual uphill filling diminishes the free surface of the melt, reducing the chances to entrap inclusions. The proposal of Campbell and colleagues is shown schematically in Fig. 5. According to these authors, the filling rate must be just enough to feed melt in front of the solidifying front at the same rate that it advances. With this configuration, the feeding necessary to compensate for the liquid to solid contraction is supplied by the incoming melt.<sup>13</sup>

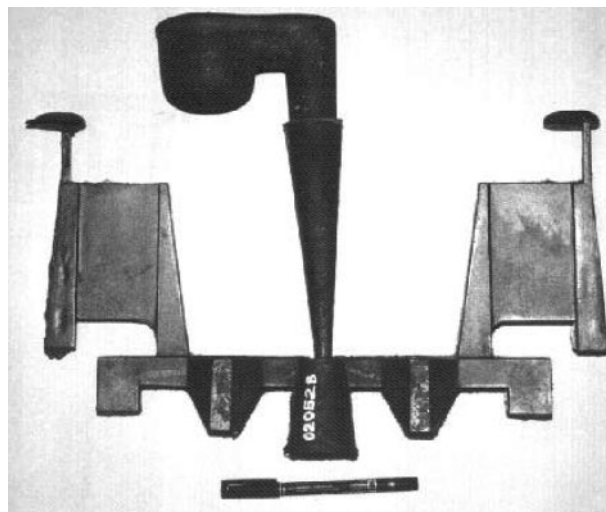
In order to design a mould that feeds the melt to the casting in the manner recommended by Campbell and colleagues, careful mathematical simulations of fluid flow were carried out using NovaFlow&Solid. This software provides detailed calculations of the melt front and flow velocity. The size and shape of all the mould components were adjusted until the desired flow and velocities were reached. Maximum admissible melt velocities were based on the proposal of Campbell,<sup>7</sup> who defines limits in the Weber number ( $We$ ), which is defined as

$$We = \frac{v^2 \rho}{\gamma/r}$$

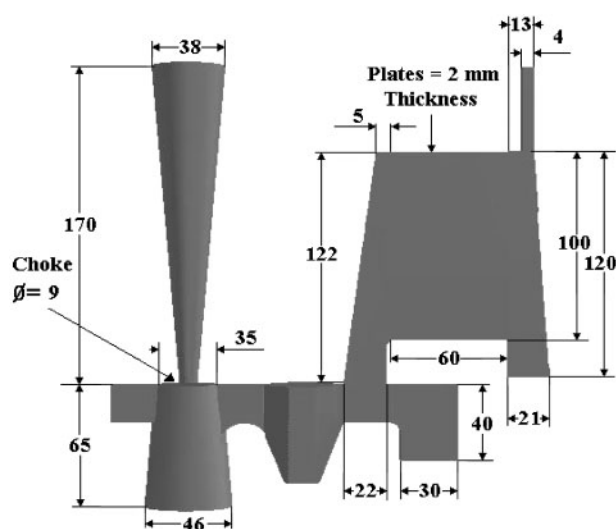
where  $v$  is the melt velocity ( $\text{m s}^{-1}$ );  $\rho$  melt density ( $\text{kg m}^{-3}$ );  $\gamma$  surface tension ( $\text{N m}^{-1}$ );  $r$  is the radius of curvature of the melt front (m); for ductile iron:  $\rho=6800 \text{ kg m}^{-3}$ ;  $\gamma=2 \text{ N m}^{-1}$  and the radius of curvature can be taken as  $r=0.5 t_n$ .

Experiments carried out on aluminium castings<sup>15</sup> showed that the melt front loses continuity when the *We* number exceeds 4.5. Assuming that this value is also valid for DI, a maximum admissible velocity of the melt can be calculated as shown in Table 4 for the flow through the 2 and 4 mm thick plates, using a *We* number value of 4.5.

The mould design included two vertical plates of 2 and 4 mm thickness. A vertical tapered runner fills each plate. Vertical channels are also placed at the external



## 6 Casting poured in vertical mould



**7 Schematic diagram of running system of vertical mould (dimensions in millimetres)**

side of each plate. The wells located at the bottom of those channels are designed to avoid back-flow, and to collect the impurities that may be present at the liquid front, which is also relatively colder. Two ceramic filters are placed in the runner system. A casting produced using the vertical mould is shown in Fig. 6.

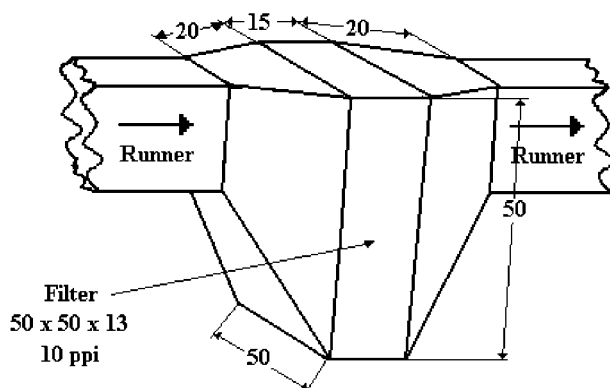
Figure 7 shows a schematic diagram of one side of the vertical mould running system including the 2 mm thickness plate.

**Table 4** Maximum admissible fluid velocity for 2 and 4 mm thick plates

| Thickness, mm | Velocity, m s <sup>-1</sup> |
|---------------|-----------------------------|
| 2             | 1.15                        |
| 4             | 0.81                        |

Table 3 Characteristic dimensions of gating system of horizontal mould

| Choke                                   | Sprue base   | Runners (2)  | Gates (8)  | Ratio of area            |
|---|--|--|--|--------------------------|
| Diam.=25 mm<br>Area=491 mm <sup>2</sup> | Diam.=70 mm<br>Area=3850 mm <sup>2</sup><br>Height=70 mm | 20 × 25 mm<br>A <sub>indiv.</sub> =500 mm <sup>2</sup><br>A <sub>total</sub> =1000 mm <sup>2</sup> | 12.5 × 10 mm<br>A <sub>indiv.</sub> =125 mm <sup>2</sup><br>A <sub>total</sub> =1000 mm <sup>2</sup> | 1:2:2<br>Non pressurised |



8 Shape and dimensions of filter chamber (dimensions in millimetres)

### Design of filter chambers

The effective area of the filter must be large enough to avoid choking the melt flow, or to be blocked by the accumulation of inclusions before pouring is complete. In order to obtain a flowrate similar to that existing in the absence of the filter, the effective area of the filter must be greater than the area of the gating system. Defining  $K$  as the ratio between the cross-sectional areas of the filter and the choke ( $K = A_f/A_c$ ), it has been shown that values of  $K < 4$  restrain the flow and make the filter work as a choke. On the other hand, if  $K$  is greater than 6, the runner controls the flowrate.<sup>16</sup> A  $K$  factor greater than 6 was achieved in both the horizontal and vertical moulds, by using two ceramic foam filters of 10 ppi and  $50 \times 50 \times 13$  mm. Figure 8 shows the shape and dimensions of the filter chamber.

### Simulation of horizontal mould casting

Figure 9 shows the simulation of fluid velocity at different stages of filling for the 1.5 and 2 mm thick plates. Figure 9a, for 74% mould filling, shows that as the liquid metal enters the thin portion of both plates, the melt front loses continuity. This is particularly noticeable on the 1.5 mm plate. This undesirable filling condition remains during the entire plate filling process, as shown in Fig. 9b and c. This is not convenient since it increases the risk of having defects in the plate. It is apparent that even though a non-pressurised configuration was adopted, the flow enters the parts in an irregular way.

Stefanescu *et al.*<sup>3</sup> have found similar flow conditions in horizontal moulds of thin plates. These observations show the risk associated with the application of empirical rules to design TWDI moulds, and highlights the potential advantages of modelling assisted design.

### Simulation of vertical mould casting

As stated above, the size and shape of the gating system of the vertical mould were designed to obtain the desired flow characteristics. Several iterations of modelling and redesigning were necessary. Figures 10 and 11 show the simulation of fluid velocity in the final design for the 2 and 4 mm thickness plates, respectively. Figure 10a, for 54% of filling of the mould, shows the effect of the filters on the flow. Figure 10b shows the flow pattern at the time the melt has filled about one-third of the plate cavity. The velocity remains below the limit of  $1.15 \text{ m s}^{-1}$  listed in Table 4. Note that the velocity

isoline of  $1.15$  is only present at the sprue basin. Figure 10c shows a smooth flow front, as the melt has nearly filled the cavity completely. The design allows the fluid velocity, at the plate cavity, to remain below the maximum admissible values listed in Table 4. Additionally, the flow follows a pattern similar to that suggested by Campbell, as desired, although some melt pours into the external channel.

Figure 11 shows that the flow patterns for the 4 mm thick plate are similar to those described for the 2 mm plate. A small region of velocities exceeding the recommended maximum velocity of  $0.81 \text{ m s}^{-1}$  (Table 4) is found at the base of the vertical channel (Fig. 11b).

Figure 12 shows the calculation of the thermal field at three different stages of filling. The temperature remains above the liquidus temperature of the alloy at every point of the casting during filling. Note that the liquidus temperature, shown by the  $1173^\circ$  isotherm is not present at any stage of filling.

### Validation of model calculations

Although the precise validation of the model calculations is difficult, some characteristics can be observed on the actual castings and compared to calculation results, such as the extent and location of shrinkage cavities, and the presence of flow marks on the casting skin that can give an indication of the actual flow pattern during filling.

Figure 13 shows the predicted shape of the melt front as it fills the 4 mm plate. Figure 14 shows flow marks found on the skin of a faulty 4 mm plate, cast at low pouring temperature. The shapes of the fronts on Figs. 13 and 14 are similar, which supports the accuracy of the model calculations.

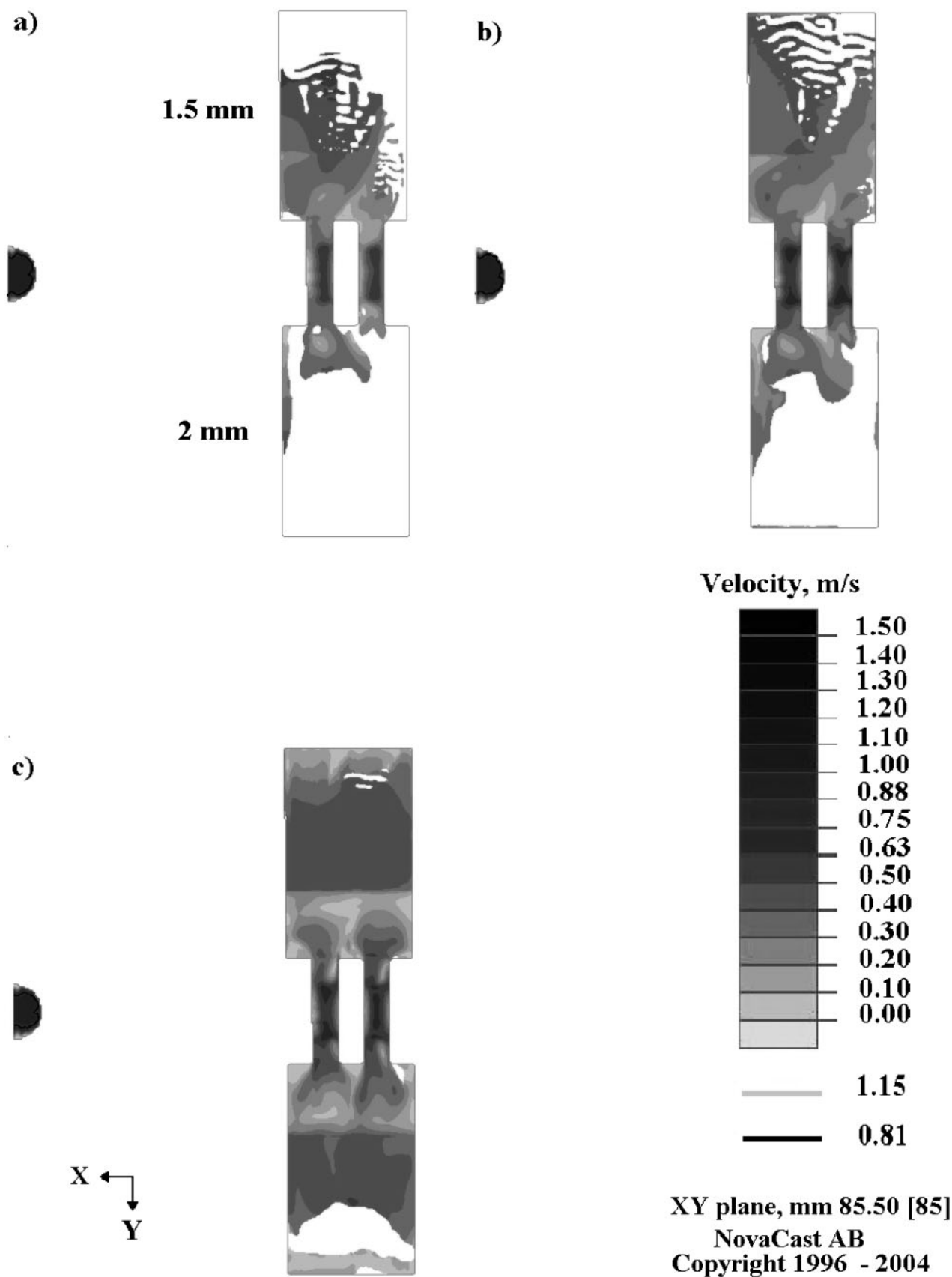
Figure 15 shows an  $xy$  cut of the horizontal mould casting. The location of the microshrinkage cavities calculated by NovaFlow&Solid, are shown in the figure as darker areas located at the triangular risers far from the ingates. Figure 16 shows the location of microshrinkage cavities on the vertical mould castings, which are present at the vertical channels that are located at each side of the plates. Figures 17 and 18 show the actual locations of the shrinkage cavities in the horizontal and vertical castings, respectively, which are in good agreement with the model calculations.

The calculations indicate that, for both the vertical and horizontal moulds, the plates are free from microshrinkage cavities. The good agreement with the observations on the castings suggests that both designs are able to produce plates free from shrinkage defects. Nevertheless, the extensive splashing observed on the calculations of flow during filling of the horizontal mould suggests that defects may be present in these plates.

The successful feeding of the thin plates in the vertical mould, in which the feeding distance is well beyond the customary limits, corroborates the validity of the procedure proposed by Campbell, and its applicability to TWDI.

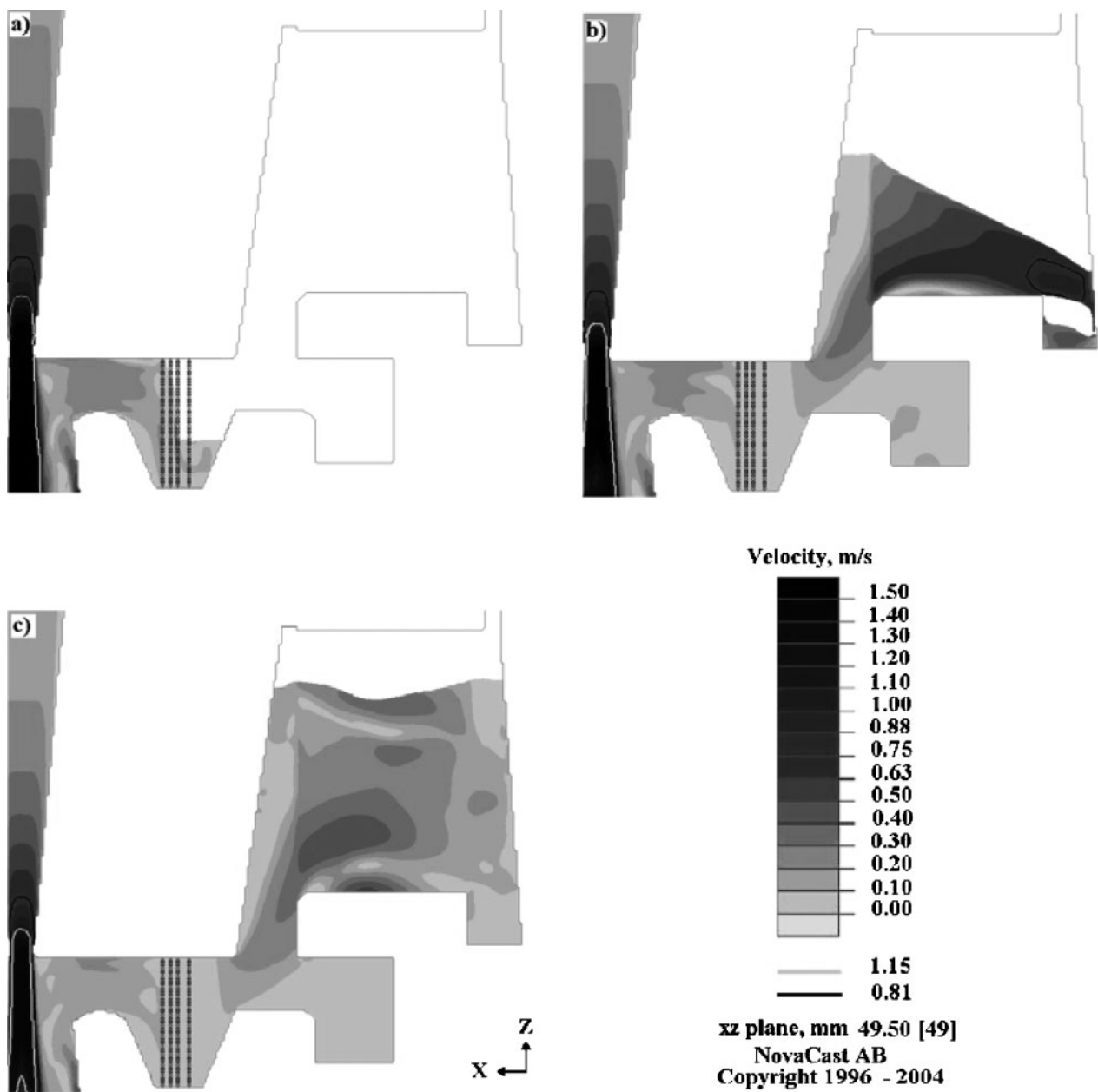
### Tensile properties and nodule counts

Tensile properties have been measured on samples of all plates as a means to evaluate the quality of the material cast using each mould. Measured values on samples of Melts A and B, listed in Table 5, are the average of at



a 74%; b 78%; c 84%

9 Simulated fluid velocity and shape of fluid front as it enters 1-5 and 2 mm thick horizontal casting blocks at different stages of mould filling



a 54%; b 86%; c 96%

10 Simulated fluid velocity and shape of fluid front as it enters 2 mm thick vertical casting blocks at different stages of mould filling

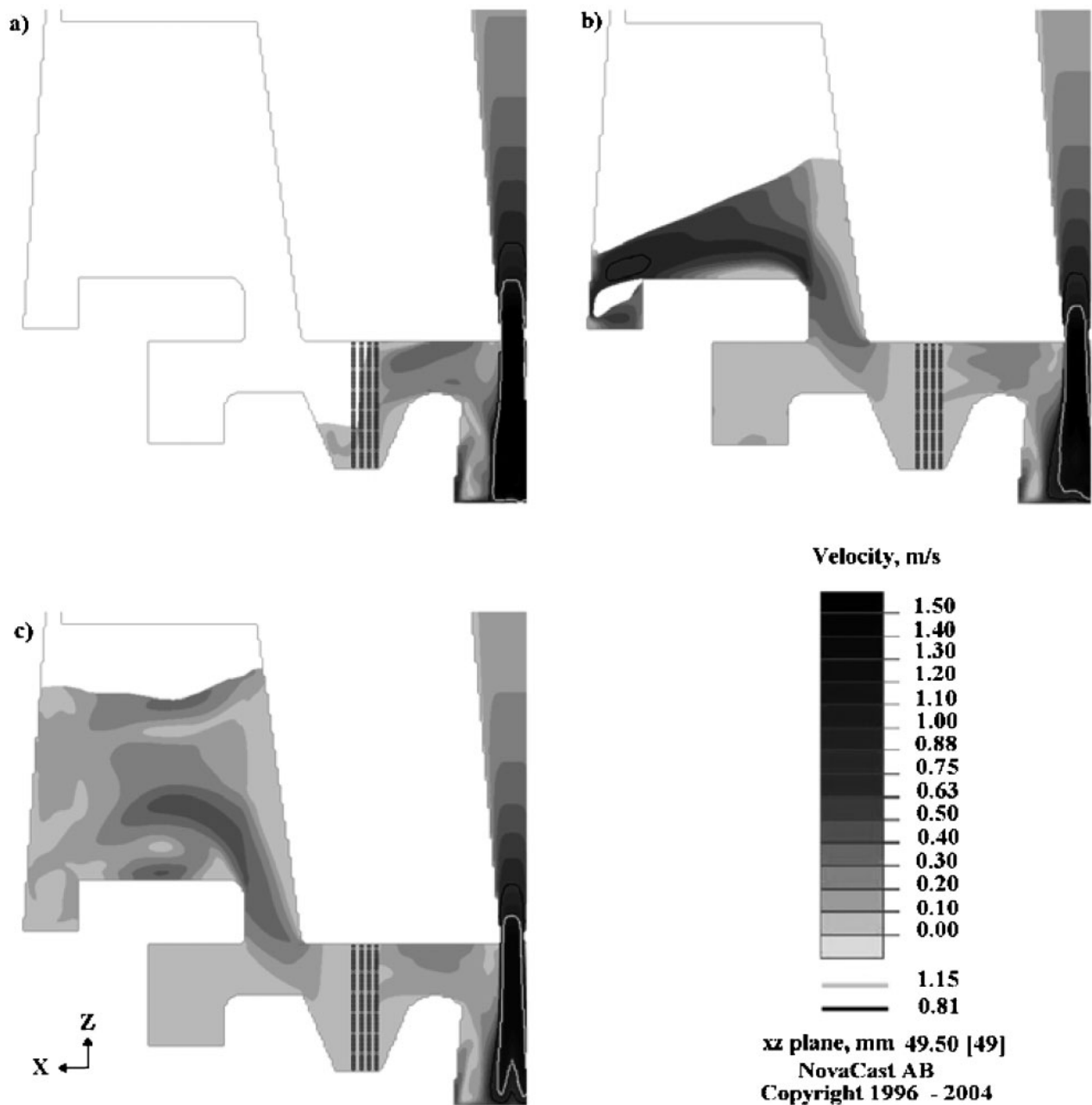
least 12 samples per experimental condition. The results include values of elongation, yield strength and UTS, and their corresponding 95% confidence interval values. For both melts and moulds, the elongation showed a significantly larger dispersion than the values of UTS and yield strength. A detailed study of the mechanical properties of TWDI has been published elsewhere.<sup>14</sup> The average UTS and yield strength values and their dispersion were similar for all samples. On the other

hand, the elongation showed small differences. Values for the samples taken from the vertical mould showed lower dispersion than those from the horizontal mould. Additionally, the elongation of samples of Melt B was lower than for samples of Melt A. This was probably caused by the higher carbon equivalent of Melt B. Earlier studies have shown that the mechanical properties of TWDI tend to decrease as the CE exceeds 4.6%.<sup>14</sup> The differences in the dispersion of the elongation of

Table 5 Mechanical properties of plates cast using vertical and horizontal moulds

| Mechanical properties | Melt A    |            | Melt B    |            | ASTM A 536 |
|-----------------------|-----------|------------|-----------|------------|------------|
|                       | Vertical  | Horizontal | Vertical  | Horizontal |            |
| Elongation, %         | 24.9±2.9  | 23.5±3.6   | 18.3±1.6  | 19.3±2.4   | 18         |
| UTS, MPa              | 454.1±5.4 | 451±7.1    | 459.1±7.5 | 453.6±3.6  | 413        |
| YS 0.2, MPa           | 288.3±3.4 | 299±8.1    | 293.4±6   | 291.2±8    | 276        |





a 54%; b 86%; c 96%

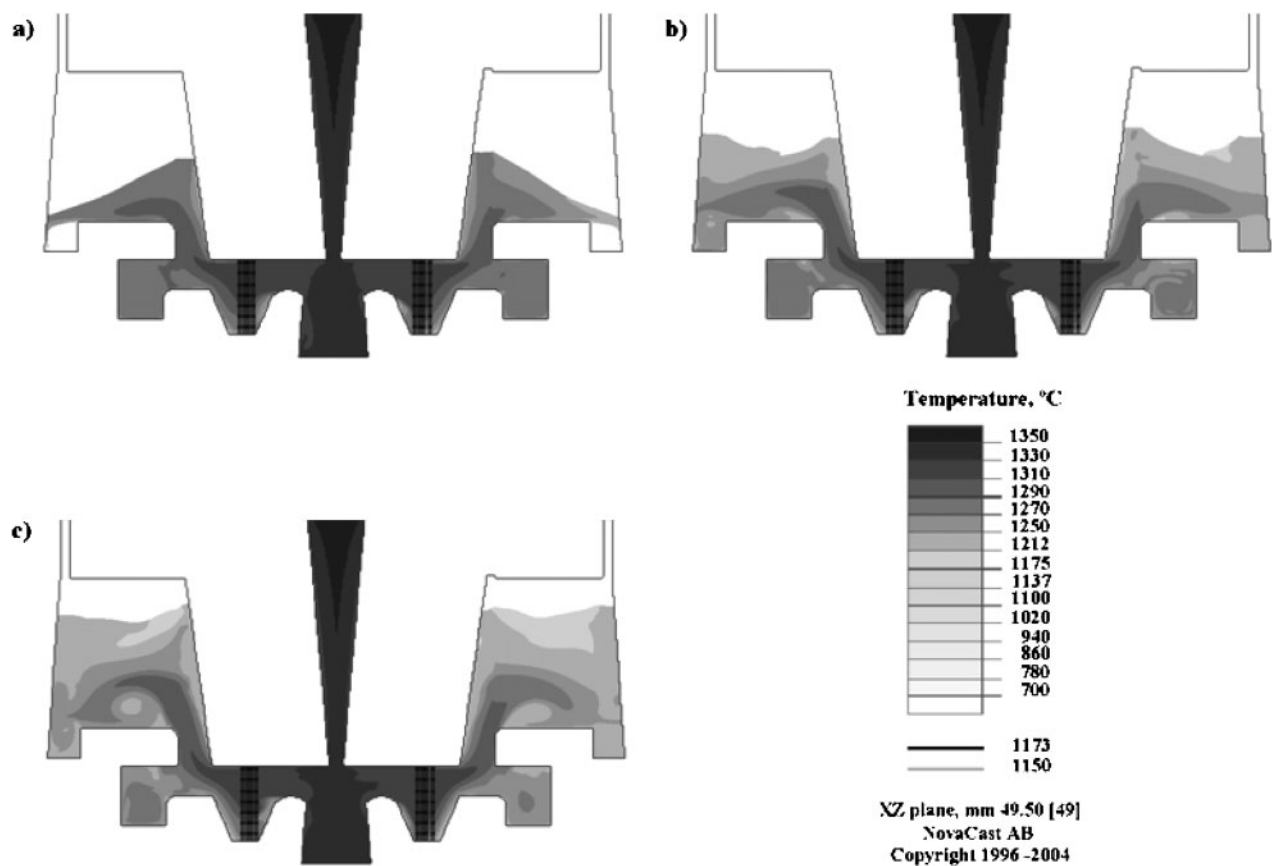
11 Simulated fluid velocity and shape of fluid front as it enters the 4 mm thick vertical casting blocks at different stages of mould filling

samples from each mould were small but significant. It must be noted that samples from vertical castings were machined from plates of  $60 \times 100$  mm, whereas those of horizontal gating design were obtained from parts with a thin section of only  $32 \times 60$  mm. The larger the plate, the higher the probability of having defects, which could impair the elongation. Most probably, the larger dispersion in the values of elongation observed on the horizontal mould was caused by defects present in the plates resulting from the irregularity of the liquid metal front as it entered the thin section, as shown by the simulation.

Table 5 lists the minimum requirements of ASTM A536. While for most cases, the average values of elongation, UTS and yield strength satisfied the minimum values of ASTM A536, this was not the case for the elongation of samples of Melt B when the dispersion

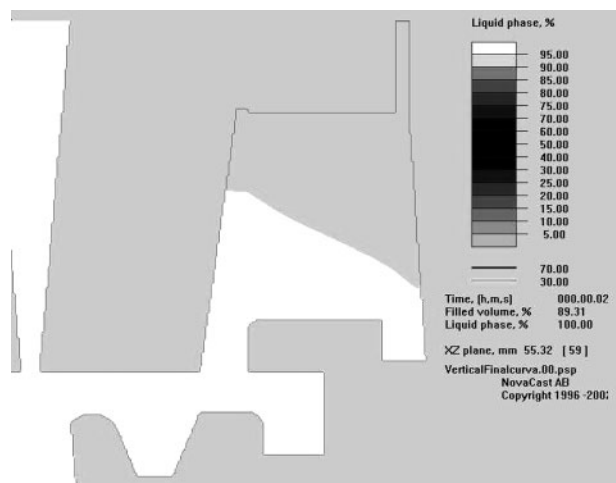
is taken into account. In fact, the bottom values of the 95% confidence interval are 16.7% and 16.9% for samples of Melt B cast in the vertical and horizontal moulds, respectively. Both values are below the lower limit of 18% in the standard.

Table 6 lists the nodule counts, sphericity and visual nodularity values. Both melts show very high nodule counts and nodularity, although on average Melt B shows greater nodule count and better nodularity than Melt A. An increase in nodule count is generally expected as the CE value increases. It is also clear that relatively small changes in thickness gave large changes in nodule counts. In addition, it is clear that similar thickness plates cast using either mould did not show the same nodule count. This suggests that, regardless of the similarity in thickness, the cooling rate during solidification was not the same. The differences in cooling rate



a 84%; b 92%; c 96%

12 Sequence of simulations of melt temperature along vertical mould for different stages of filling



13 Simulated morphology of fluid front as it fills 4 mm thick vertical plate

were also reflected in the software calculations. This fact emphasises the limited applicability of rules based solely on thickness or modulus, and stresses the importance of detailed calculations of solidification using software. The differences in cooling rate are the result of different local feeding temperatures. Despite having the same pouring temperature, the metal feeding the thin sections has different temperatures in each case, since its flow through the two different feeding systems results in different heat losses.

Skin roughness

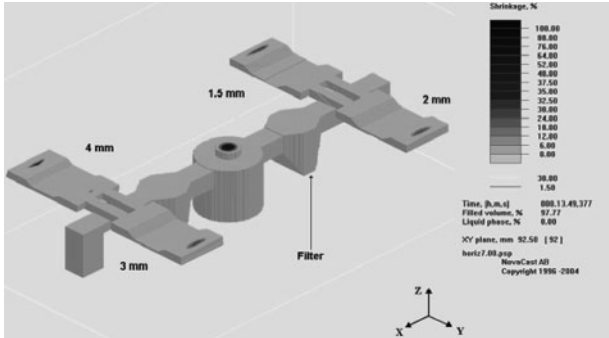
The roughness of the casting surface can have a marked effect on the mechanical performance of TWDI parts. The volume fraction affected by the surface increases as the thickness of a given part decreases, augmenting the influence of surface topography on mechanical properties such as tensile strength, ductility and fatigue strength. Although this effect could not affect the

Table 6 Nodule counts, sphericity and visual nodularity for Melts A and B

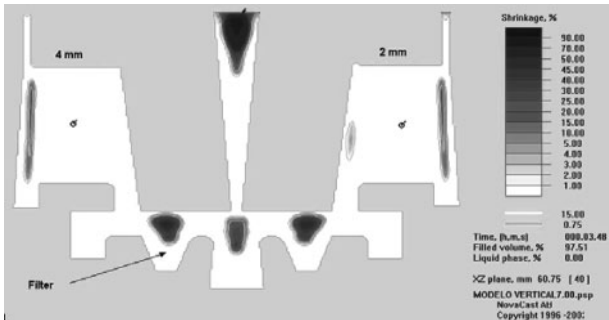
| Plate             | Nodule counts, Nod mm <sup>-2</sup> |        | Sphericity |        | Visual nodularity, % |        |
|-------------------|-------------------------------------|--------|------------|--------|----------------------|--------|
|                   | Melt A                              | Melt B | Melt A     | Melt B | Melt A               | Melt B |
| Vertical 2 mm     | 1899                                | 2000   | 0.67       | 0.74   | 100                  | 100    |
| Vertical 4 mm     | 1194                                | 1090   | 0.65       | 0.72   | 90/80                | 100/90 |
| Horizontal 1.5 mm | 1891                                | ...    | 0.70       | ...    | 100                  | ...    |
| Horizontal 2 mm   | 1272                                | 1552   | 0.68       | 0.78   | 100/90               | 100    |
| Horizontal 3 mm   | 1164                                | 1413   | 0.67       | 0.76   | 90                   | 100/90 |
| Horizontal 4 mm   | 970                                 | 980    | 0.67       | 0.72   | 90/80                | 90     |



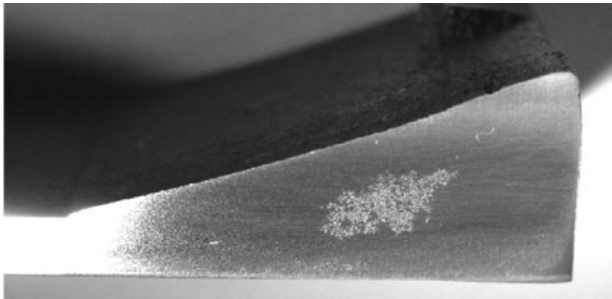
14 Plate of 4 mm thickness cast in vertical mould showing surface defect; ruler shows dimensions in centimetres



15 Location of shrinkage cavities in horizontal casting as predicted by simulation software; cavities are shown as dark areas



16 Location of shrinkage cavities in vertical casting as predicted by simulation software; cavities are shown as grey patches

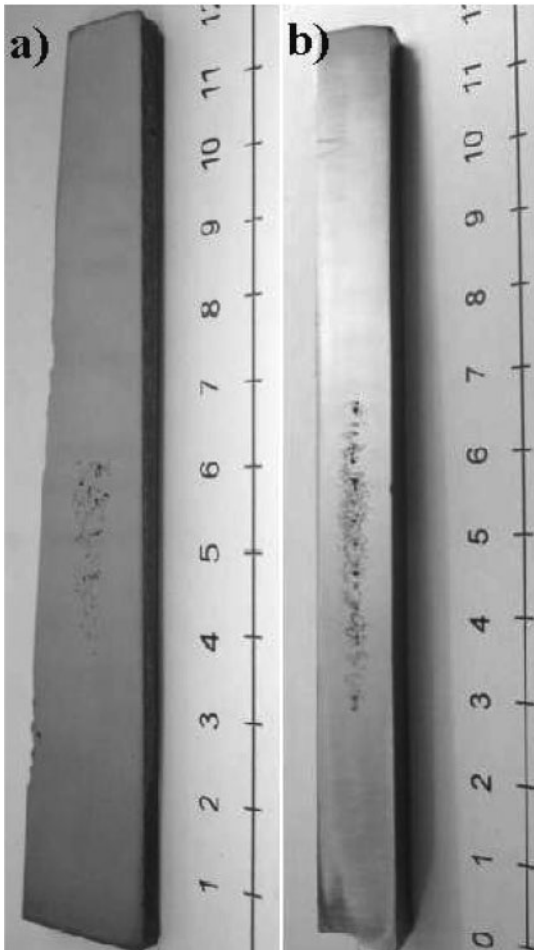


17 Polished section through wedged portion of horizontal casting, showing location of microshrinkage

mechanical properties measured in the present study since the skin was removed by grinding, the surface roughness of the castings was measured as a means to characterise the surface quality.

The typical skin roughness values for sand castings are in the range of 6.3–50  $\mu\text{m}$ .<sup>17</sup> The most frequent values range between 12.5 and 25  $\mu\text{m}$ .<sup>17</sup>

Table 7 lists  $R_a$  values measured on the 2 and 4 mm thickness plates, cast using the horizontal moulds. The values for the bottom sides of the plates are near 10  $\mu\text{m}$ , which represents a smoother finish than the average sand casting, whereas the top side of the plates showed values of up to 18  $\mu\text{m}$ , close to the usual average for sand castings.



a longitudinal cut; b transversal cut

18 Polished section through vertical channel that feeds metal into vertical plates showing microshrinkage cavities; ruler shows dimensions in centimetres

**Table 7 Surface roughness of plates cast using horizontal mould**

| Mould      | Thickness, mm | Face   | $R_{a, \mu m}$   |
|------------|---------------|--------|------------------|
| Horizontal | 2             | Top    | $18.15 \pm 1.65$ |
| Horizontal | 2             | Bottom | $10.80 \pm 1.21$ |
| Horizontal | 4             | Top    | $11.35 \pm 1.15$ |
| Horizontal | 4             | Bottom | $9.38 \pm 0.25$  |

## Conclusions

1. A horizontal mould was designed to cast thin wall plates of ductile iron using a non-pressurised configuration. The design was based on empirical rules and previous experience. The ability of the mould to fill the plate cavity with low surface turbulence was verified using the software NovaFlow&Solid. The results show that the adoption of empirical rules and a non-pressurised configuration are not enough to guarantee proper filling, since extensive splashing and an excessive flow velocity were found.

2. A vertical mould was designed to cast thin wall plates of ductile iron using a non-pressurised configuration. The design procedure applied mathematical modelling of fluid flow combined with limits of flow velocity calculated on the basis of the Weber number. The mould was capable of producing sound TWDI plates.

3. Mathematical modelling of both the vertical and horizontal moulds using NovaFlow&Solid simulation software was able to predict with accuracy the location and size of the microshrinkage cavities.

4. The vertical mould design used vertical feeders along the sides of the thin wall plates. Through this design, a low turbulence uphill filling was obtained.

5. Tensile testing of samples taken from the two moulds showed less dispersed results for the vertical mould, probably as a result of the irregular flow front found in the horizontal mould filling.

## References

1. A. Giacomini, R. Boeri and J. Sikora: *Mater. Sci. Technol.*, 2003, **19**, 1755–1760.
2. D. M. Stefanescu, L. P. Dix, R. Ruxanda, C. Corbitt-Coburn and T. S. Piwonca: *AFS Trans.*, 2002, **110**, 1149–1161.
3. D. M. Stefanescu, R. Ruxanda and L. P. Dix: *Int. J. Cast Met. Res.*, 2003, **16**, 319–324.
4. A. Javaid, J. Thomson, M. Sahoo and K. G. Davis: *AFS Trans.*, 2001, **109**, 1–18.
5. A. Javaid, J. Thomson, M. Sahoo and K. G. Davis: *AFS Trans.*, 1999, **107**, 441–456.
6. J. G. Sylvia: 'Cast metals technology', 175–195; 1972, Lakeville, MA: Addison-Wesley Publishing Co.
7. J. Campbell: 'Castings', chapters 2 and 5; 1991, Linacre House, Jordan Hill, Oxford, Butterworth-Heinemann Ltd.
8. J. P. LaRue: 'Basic metalcasting', 91–109; 1989, Des Plaines, IL, USA, American Foundrymen's Society, Inc.
9. C. Labrecque and M. Gagné: *AFS Trans.*, 2000, **108**, 31–38.
10. F. Mampaey and Z. A. Xu: *AFS Trans.*, 1997, **105**, 95–103.
11. C. Labrecque, M. Gagné, A. Javaid and M. Sahoo: *Int. J. Cast Met. Res.* 2003, **16**, 313–317.
12. A. Javaid, K. G. Davis and M. Sahoo: *AFS Trans.*, 2000, **108**, 191–200.
13. J. Campbell: *Mater. Sci. Technol.*, 1988, **4**, 194–204.
14. P. David, J. Massone, R. Boeri and J. Sikora: *ISIJ Int.*, 2004, **44**, 1180–1187.
15. J. Runyoro, S. Boutorabi and J. Campbell: *AFS Trans.*, 1992, **100**, 225–234.
16. Y. Yang, H. Nomura and M. Takita: *Int. J. Cast Met. Res.*, 1996, **1**, 27–35.
17. ASM Handbook: 'Surface engineering', vol. 5, 147; 1994, ASM International.

Copyright of International Journal of Cast Metals Research is the property of Maney Publishing and its content may not be copied or emailed to multiple sites or posted to a listserv without the copyright holder's express written permission. However, users may print, download, or email articles for individual use.